SYNTHESIS OF NANOCOMPOSITE MATERIALS BASED ON TiO_2 NANOTUBES AND POLYMETHYLENE NAPHTHYLENE SULFONATE AND THEIR ELECTROPHYSICAL PROPERTIES

Sh. Djumagulov[1], B. Umarov[1], A. Khamidov[2], O. Ruzimuradov[2], A. Kenjaev[3]

[1]National University of Uzbekistan, Universitet 4, Tashkent, Uzbekistan 100174
[2]Turin Polytechnic University in Tashkent, Kichik khalqa yuli 17, Tashkent 100095
[3]Academic Lyceum of Jizzakh State Pedagogical University (Sailjoyi), Jizzakh city

Received 11.06.2025
Accepted 18.09.2025

Abstract: *In this study, nanocomposite materials based on titanium dioxide and polymethylene naphthalene sulfonate (PMNS) were investigated. The main objective was to evaluate the enhancement in ionic conductivity of the synthesized TiO_2/PMNS nanocomposites. Key structural parameters—including nanotube diameter, wall thickness, and pore spacing—were measured and statistically analyzed. The experimental results demonstrated that well-ordered titanium dioxide nanotubes were successfully formed at 25 °C from an electrolyte containing 0.5 M ammonium fluoride (NH_4F/EG/H_2O) under an applied voltage of 60 V. The surface morphology of the nanotubes was characterized using scanning electron microscopy (SEM), and their chemical structure was examined by IR spectroscopy. Polymethylene naphthalene sulfonate was synthesized using naphthalene as the starting material. The reaction conditions were optimized, and the molecular structure of the resulting sulfonated compounds was analyzed through quantum chemical calculations. Variation of water content in the electrolyte (2, 10, and 45 %) significantly affected the ionic conductivity of the TiO_2/PMNS nanocomposites. Materials synthesized from an electrolyte containing 2 % H_2O at 25 °C exhibited the highest ionic conductivity.*
Key words: *anodizing, ammonium fluoride, water, pore diameter, naphthalene, polymethylene naphthalene sulfonate, electrical conductivity.*

Introduction

In recent years, TiO_2 nanotubes have attracted significant attention from both the scientific community and industry due to their semiconducting behavior and a wide range of functional properties. Porous anodic oxides—such as porous aluminum [1], titanium dioxide nanotubes, and other related nanostructured materials—are of considerable research interest, since nanostructures derived from them serve as valuable components in numerous technological fields. In particular, anodic titanium oxide nanotubes (ATO) are widely explored for applications in solar energy conversion, supercapacitors, sensors, catalytic systems, and other advanced technologies [2]. A. Khamidov and his research team synthesized nanostructured anodic aluminum oxide (AAO) membranes using oxalic acid as the electrolyte through a two-step anodization process. They examined the influence of electrolyte temperature on pore formation in AAO membranes and investigated the catalytic activity of nanocatalysts prepared by incorporating various metal nanoparticles into the pores [3, 4].

Habasaki and others, based on numerous experiments, studied the arrangement of titanium dioxide NTs (nanotubes) in a hexagonal pattern [5]. Naphthalenesulfonic acids have the general formula $C_{10}H_{8-n}(SO_3H)_n$ and are colorless or light-yellow crystalline compounds. They are readily soluble in ethanol, diethyl ether, concentrated mineral acids, and water. According to theoretical predictions, sulfonation of naphthalene may yield 2 monosulfonic, 10 disulfonic, 14 trisulfonic, and 22 tetrasulfonic acids. However, in practice the number of isolable isomers is considerably lower: only 2 monosulfonic, 6 disulfonic, 3 trisulfonic, and 1 tetrasulfonic acid are typically obtained [6]. When sulfonation is conducted at low temperatures (around 80 °C), the predominant product is 1-naphthalenesulfonic acid because the activation energy for its formation is lower than that for 2-naphthalenesulfonic acid. At higher temperatures (approximately 160 °C), the reaction approaches equilibrium more rapidly, resulting in the conversion of 1-naphthalenesulfonic acid into 2-

naphthalenesulfonic acid. Importantly, this transformation is not a direct isomerization; rather, it proceeds through desulfonation followed by hydrolytic elimination of the sulfo group and subsequent re-sulfonation of the naphthalene ring [7]. Electrically conductive nanocomposite materials incorporating organic and inorganic phases are extensively used in electrical engineering and high-tech applications, including electroluminescent diodes, thin-film transistors, sensors, electronic displays, digital memory and logic devices, solar cells, solid-state batteries, and medical diagnostic and analytical systems requiring high precision [8–11].

Our objective is to develop hybrid materials combining inorganic and organic components and to identify their potential fields of application, which are gaining increasing global relevance. In this study, nanocomposite materials based on the inorganic compound titanium dioxide and the organic compound polymethylenenaphthalene were synthesized. Their electrical conductivity and volt-ampere characteristics were systematically investigated to evaluate the functional performance of the resulting hybrid structures.

Experimental part

Materials and methods. Titanium foil (99.9% pure, Beantown Chemical) was used in this study. The foil was cut into 3 cm^2 sections and was 0.2 mm thick. Since the foil had various roughnesses and inclusions on the surface, it was first cleaned sequentially in acetone, isopropyl alcohol, and distilled water (ultrasonic clean GT Sonic-D 6, AC-220-240V) for 12 min and then air-dried for 1.5 h. After that, an electrolyte solution containing 2% deionized water, 97.5% ethylene glycol, and 0.5 g ammonium fluoride (NH_4F) was prepared for the anodization process.

The cleaned and dried titanium foil was connected to the anode of a vertical electrolytic cell, and the opposite electrode was connected to the graphite cathode. The voltage was sequentially applied from 20 to 80 V (Corrtest CS 350M, China). The anodizing time was between 4 and 6 hours, and each process was repeated three times [12].

Results and discussion

The formation of TiO_2 nanotubes depends on multiple parameters, one of the key factors being the chemical aggressiveness of the electrolyte. The dissolution of intermediate titanium oxofluorides formed between tube walls is essential for the transition from nanopores to well-defined nanotubular structures.

Nanotubes were synthesized at different anodization voltages (20, 40, 60, and 80 V) using a Corrtest CS 350M (China) power supply. The voltammetric behavior of fluoride (F^-) and oxygen (O^{2-}) anions during oxidation is shown in Figure 1a. At 20 V, the oxidation current initially reached 57 mA at 5 s and decreased to 36.8 mA at 8.7 s, indicating the onset of pore formation. An oxide layer was completed at 49.7 mA at 18 s, after which the process continued at a stable current density. At 40 V, the oxidation current began at 42.4 mA at 4 s, decreased to 31.2 mA at 9.1 s, and reached 45.3 mA at 25.9 s, maintaining a constant current thereafter. The final current exceeded the initial value (45.3 mA > 42.4 mA), confirming the growth of a denser oxide layer. At 60 V, the oxidation process started at 32.7 mA at 4 s, dropped to 24.6 mA at 5.6 s, and ended at 45.3 mA at 52.9 s. The difference between the initial and final currents (ΔI = 12.6 mA) indicates an efficient oxidation process and formation of an organized oxide layer. At 80 V, the process began at 25.3 mA at 2.8 s, decreased to 17.6 mA at 2.6 s, and reached 41.3 mA at 98.9 s. However, SEM analysis revealed that nanotubes formed at this voltage were less ordered and characterized by excessive diameter, likely due to excessive chemical dissolution. Based on the voltammetric profiles and morphological observations, the nanotubes synthesized at 60 V exhibited the highest degree of order and uniform hexagonal geometry (Fig. 1a). This optimal structure correlates with the balanced dissolution and oxidation rates reflected in the ΔI value of 12.6 mA.

Based on the voltammetric characteristics, it can be concluded that among the nanotubes synthesized at different anodization voltages, the structures formed at 60 V exhibit the highest degree

of ordering and well-defined hexagonal geometry (Fig. 1a). This conclusion is supported by the difference between the initial oxidation current and the current measured at the point of oxide-layer formation ($\Delta I = 12.6$ mA), which reflects a balanced relationship between oxide growth and chemical dissolution processes.

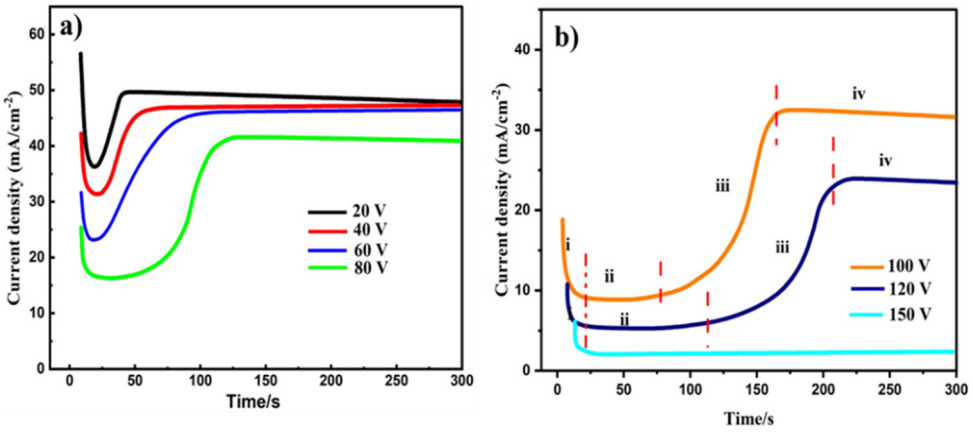

Fig. 1. Time-dependent voltammetric characteristics of current at (a) 20, 40, 60, and 80 V and (b) 100, 120, 150 V

A characteristic feature of well-ordered nanotube formation is that the initial current value supplied by the potentiostat is higher than the current measured at the stage of oxide-layer development. This indicates controlled and uniform nanotube growth. In contrast, increasing the applied voltage to 100, 120, and 150 V results in more aggressive oxidation and the formation of a thicker oxide layer; however, the resulting nanotubes are irregular and poorly ordered. In these cases, the initial current values are lower than the current values during the oxidation stage, indicating unstable growth dynamics and disordered structural development (Fig. 1b).

Thus, 60 V was determined to be the optimal anodization voltage for obtaining uniform and highly ordered TiO_2 nanotube arrays.

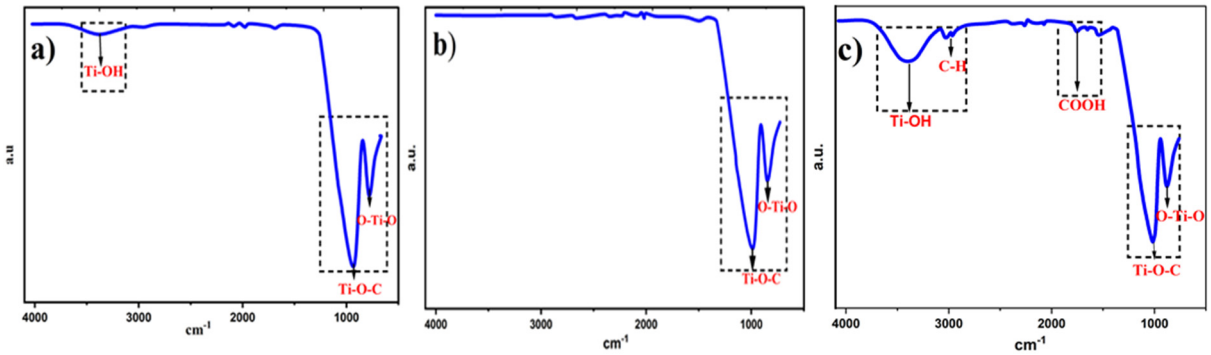

Fig. 2. IR spectrum of titanium dioxide TiO_2 nanotubes obtained after anodization

During the formation of nanotubes, fluoride ions (F^-) in the solution combine with (Ti^{+4}) ions emerging from the metal layer to form $[TiF_6]^{-2}$ salt, and samples (IR-infrared spectroscopy) were taken to determine whether fluoride ions are present in these formed nanotubes (Fig. 2a-c). If the electrolyte is neutralized with alkali to change its acidity, it can be seen that the acidity of the medium decreases, the alkalinity increases, and the resulting nanotubes are formed (Fig. 2a).

In addition, in order to increase the acidity of the solution, the anodizing process was also carried out in an acidic environment in order to accelerate the dissolution of the titanium foil and the formation of an oxide layer by reducing the barrier layer. In Fig. 2b, it can be seen that the environment is neutral. From Fig. 2c, it can be seen that the increasing acidity of the solution and the formation of highly ordered nanotubes in the hexagonal state nanotubes were formed.

Formation of nanotubes. As shown in Fig.s 3a–b, double-walled nanotubes with a uniform, flat surface and a high degree of ordering were successfully obtained. The formation of double-walled structures is associated with the migration of fluoride ions (F^-) into the growing oxide layer and their interaction with titanium ions (Ti^{4+}) originating from the metallic substrate. This process results in the formation of water-soluble titanium hexafluoride complexes. Subsequent dissolution of these complexes within the inner region of the oxide layer leads to the development of an additional wall structure, ultimately producing a double-walled nanotube morphology.

The top SEM (SEM SUPRA 40, Carl Zeiss) and elemental composition of the nanotubes formed in the highly ordered hexagonal state are shown in Figs. 3a and 3b. The elemental composition of nanotubes is as follows: 65.55% Ti, 31.45% O, and 3% C. From this it can be concluded: the higher the amount of titanium and oxygen in the formation of the oxide layer compared to the initial oxide layer, the faster the formation of the oxide layer. This occurs under the influence of the electrostatic field of the ions in the solution; that is, the positive and negative ions combine with each other under the influence of electrostatic force, forming a chemical process.

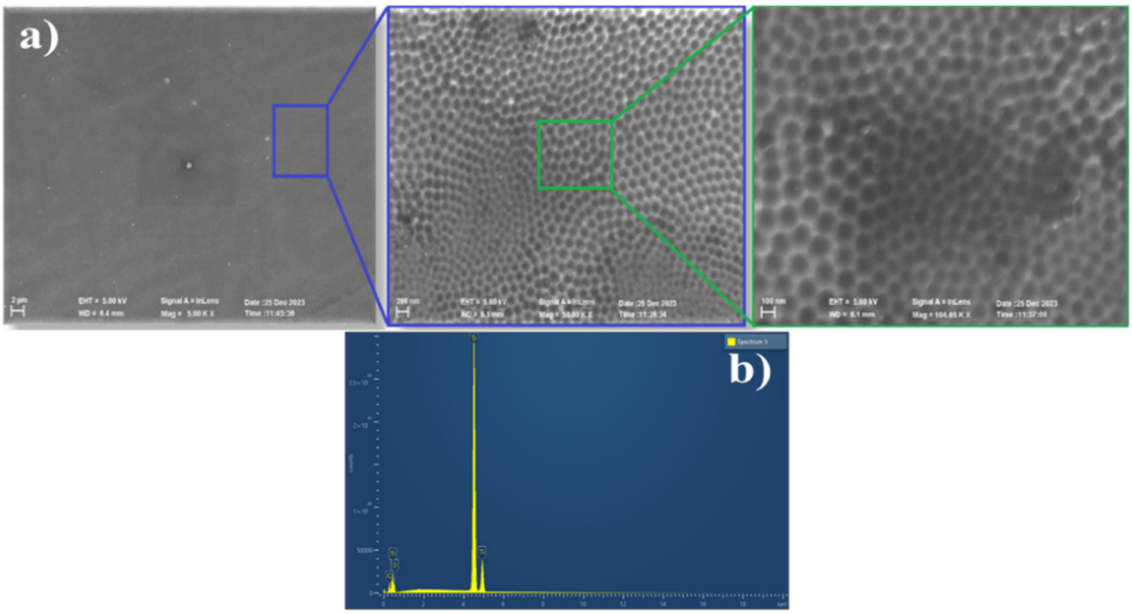

Fig. 3. SEM-EDS (a) and (b) micrographs of nanotubes obtained at 20 ºC, 60 V with 0.5% NH_4F

1. Synthesis of polymethylene naphthalene sulfonate (PMNS). The process of obtaining the copolymer product consists of the following steps:

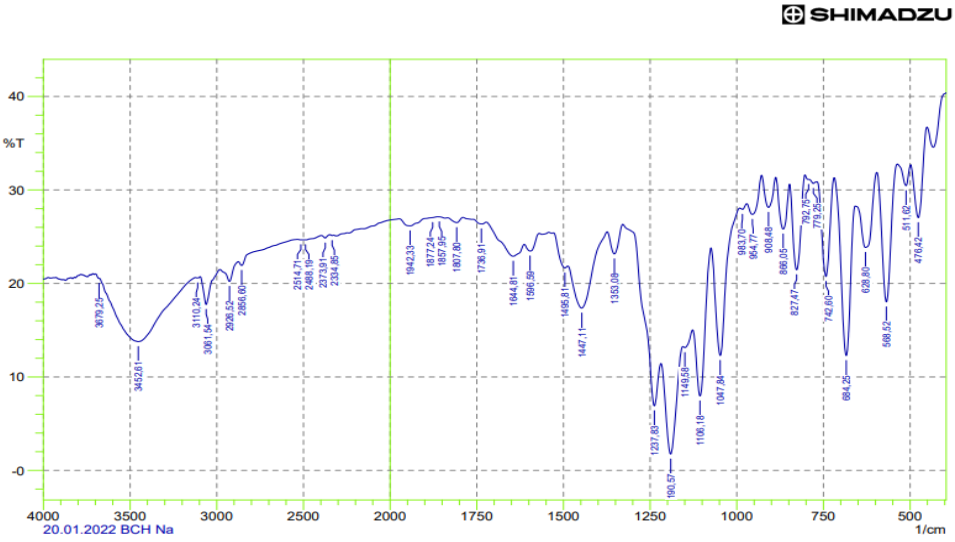

Fig. 4. IR spectrum of 2-sulfonaphthalene

Naphthalene sulfonation process: naphthalene and sulfuric acid at a 1:1.2 molar ratio and a temperature of 160ºC for 8 hours yielded 2-sulfonaphthalene with a yield of 89%. Increasing the reaction time in the process of obtaining 1- and 2-naphthalenesulfonic acids caused a decrease in their yield. In this case, the occurrence of additional reactions leads to a decrease in the yield of the product [13].

The valence vibrations of the -C-H group can be observed in the region frequency of 3061.54 cm^{-1}, the valence vibrations of the C=C bond in the aromatic nucleus in the region of 1596.59 cm^{-1}, the valence vibration of the aromatic nucleus in the region of 742.6 cm^{-1}, the valence vibrations of the $-SO_3H$ group in the region of 1106.18 cm^{-1} and the valence vibrations of the C=O bond in the region of 1190.57 cm^{-1} [12].

2. Polycondensation of 2-naphthalenesulfonic acid with formalin (35%). The process was carried out at high pressure in a hydrothermal reactor. Initially 2-naphthalenesulfonic acid and formaldehyde were taken at a 1:2 molar ratio, and the process was carried out at 90-100°C for 6 hours. Polymethylenenaphthalenesulfonic acid was obtained with a yield of 92.4%. The polycondensation reaction was carried as follows:

Process mechanism:

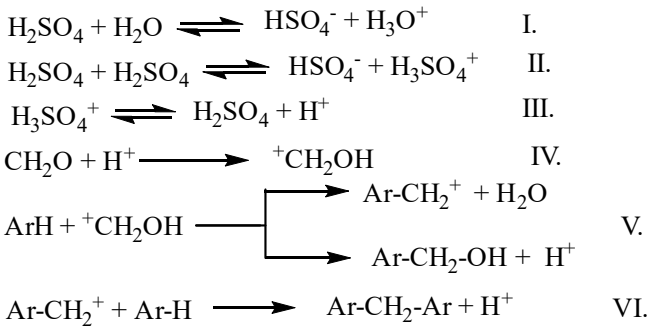

In order to theoretically determine the occurrence of the above chemical processes, the results of quantum chemical calculations were analyzed using the Gauss-09 program.

Initially, the charge distribution, bond lengths, HOMO, LUMO values and electrostatic charge distribution values of the naphthalene molecule were calculated.

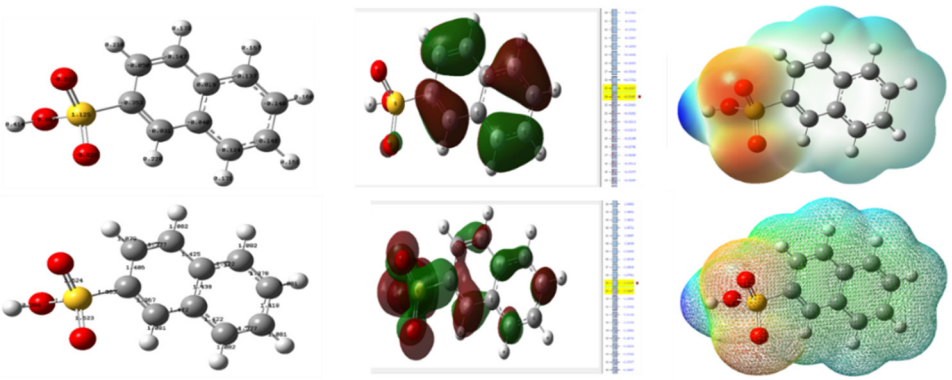

Fig. 5. Charge distribution, bond lengths, HOMO, LUMO values, and electrostatic charge distribution in the sulfonnaphthalene molecule

If we pay attention to these quantum chemical calculations, it can be shown that there is an over-distributed charge distribution in the analytically active sulfo group in the naphthalene molecule (Fig. 5).

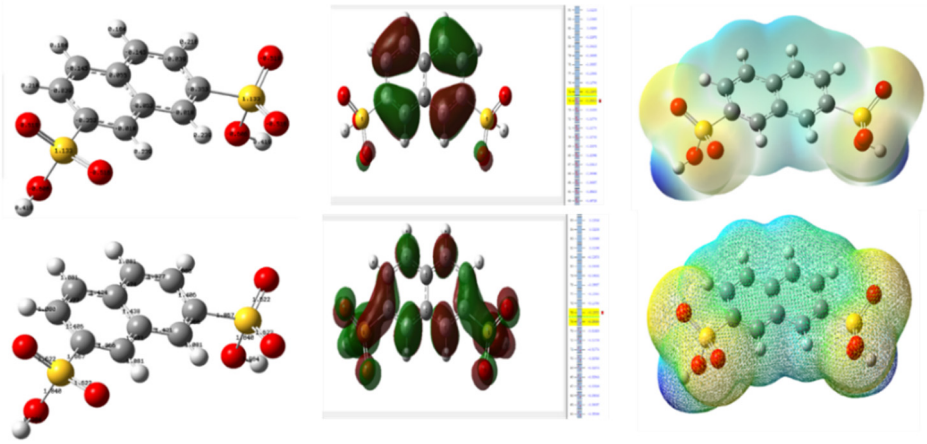

Fig. 6. Charge distribution, bond lengths, HOMO, LUMO values and electrostatic charge distribution in the disulfonaphthalene molecule

In this case, the analytically active sulfo groups in the disulfonaphthalene molecule possess an excess electron density, which enables them to participate in reactions through these reactive sites (Fig. 6). The morphology, surface structure, and elemental composition of the spatially structured PMNS were analyzed. The development of the three-dimensional (spatial) structure is attributed to the high formalin content generated during the polycondensation process, the large number of methoxy groups in the intermediate product, and the subsequent thermal treatment at elevated temperatures, which promotes structural cross-linking.

SEM images of polymethylenenaphthalenesulfonic acid are shown in Fig.s 7c–d. The micrographs reveal the presence of macropores ranging from 114 to 613 μm, indicating that adsorption processes may occur within these pores. Elemental analysis shows that the polymer consists predominantly of carbon (68.3%) and oxygen (18.1%).

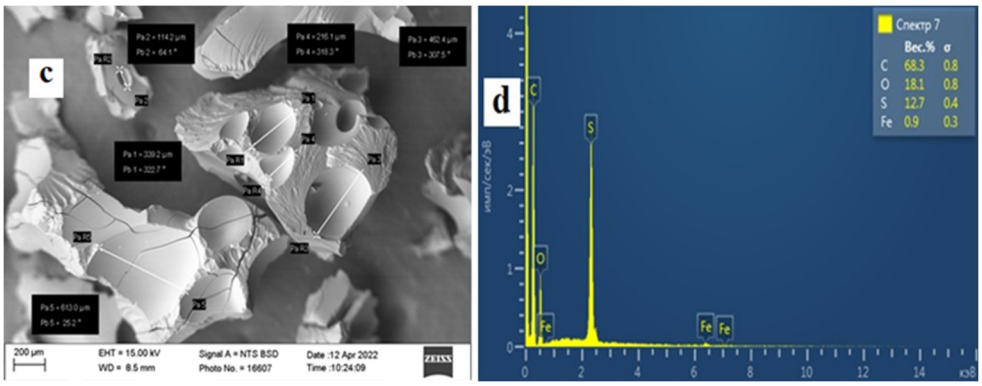

Fig. 7. SEM-EDS analysis of polymethylenesulfonatenaphthalene (c-d).

3. Obtaining nanocomposite materials and their physico chemical characteristics. The nanocomposite materials were synthesized by incorporating polymethylenenaphthalenesulfonate (PMNS) monomers into pre-formed titanium dioxide nanotubes using an electrochemical deposition method. The process was performed as follows: titanium oxide nanotube samples with an area of 2 cm^2 (1 × 2 cm) were connected to the anode of an electrochemical cell, and an electrolyte consisting of 10 g of polymethylenenaphthalenesulfonate dissolved in 100 g of DMSO was introduced into the system. A platinum electrode was used as the counter (cathode) electrode. The electrolysis process was carried out for 1 hour, resulting in the formation of TiO_2/PMNS nanocomposite materials. The

progress of each stage was monitored, and the final morphology was examined using SEM, as shown in [14].

To investigate the influence of monomer concentration, electrolysis was performed in supersaturated, saturated, and unsaturated solutions of polymethylenenaphthalenesulfonate. In the supersaturated solution, SEM analysis showed that absorption occurred predominantly on the outer surface of the nanotubes due to the high concentration of monomer ions, which limited penetration into the tubes. In contrast, electrolysis in the saturated solution resulted in uniform deposition of monomer ions on the surface, inside the nanotube channels, and along the tube walls. In the case of the unsaturated solution, the low concentration of monomer ions led to weak absorption and minimal incorporation into the nanotube structure.

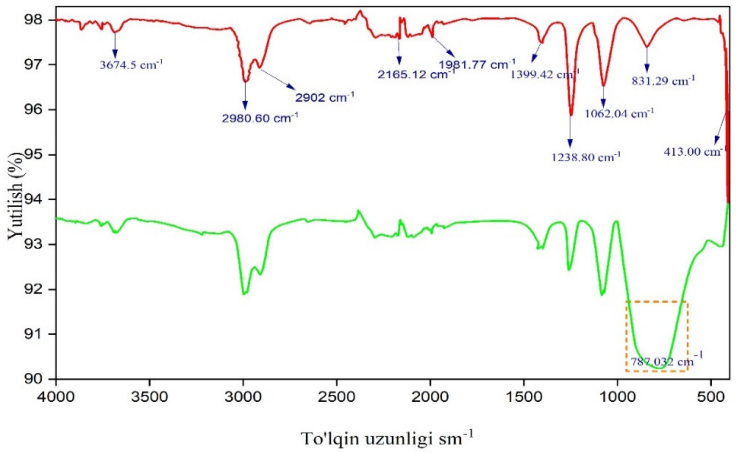

Fig. 8. IR spectrum of titanium dioxide nanotubes TiO_2 and TiO_2/PMNS nanocomposites

The vibration frequency is 787.3 cm^{-1}, the valence vibrations of the -Ti-O bond in the aromatic core, 2980.60 cm^{-1}, the valence vibrations of the C=C bond in the aromatic core, 1062.04 cm^{-1}, the valence vibrations of the -SO_3H group, and 1238.80 cm^{-1}, the valence vibrations of the C=O bond can be observed.

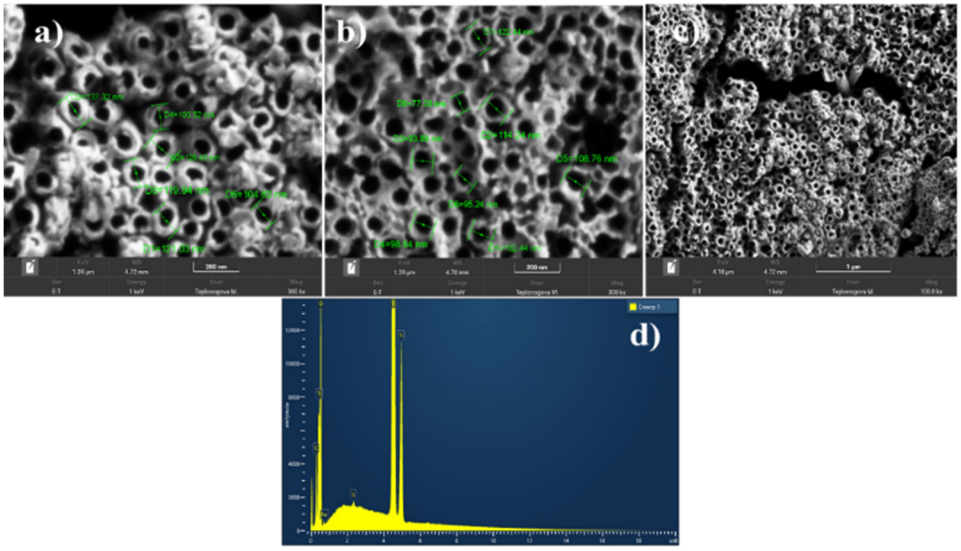

Fig. 9. (a-c) SEM and EDS analysis micrographs of the obtained nanocomposites (electrolyte containing 45, 10 and 2% water

Fig. 9a shows a top-view SEM micrograph of a nanocomposite obtained from an electrolyte containing 2% water. Nanocomposites containing 2% water differ in oxide layer thickness compared to nanocomposites containing 10 and 45% water. It can be seen that the polymethylene naphthalene

sulfonate monomers are adsorbed to the interior, sides, and surface of the pores. The nanocomposites with 10% water in the electrolyte have a larger diameter, which also indicates that the above polymethylenenaphthalene sulfonate monomers are more adsorbed on the interior, side, and surface of the pores (Fig. 9b).

It is evident from the SEM images that the nanocomposites with 45% water in the electrolyte have a much larger diameter, which indicates that the adsorption process is higher than that of the remaining nanocomposites. The volt-ampere characteristics of the resulting nanocomposites were studied over range of voltages 0 to 1.5 V.

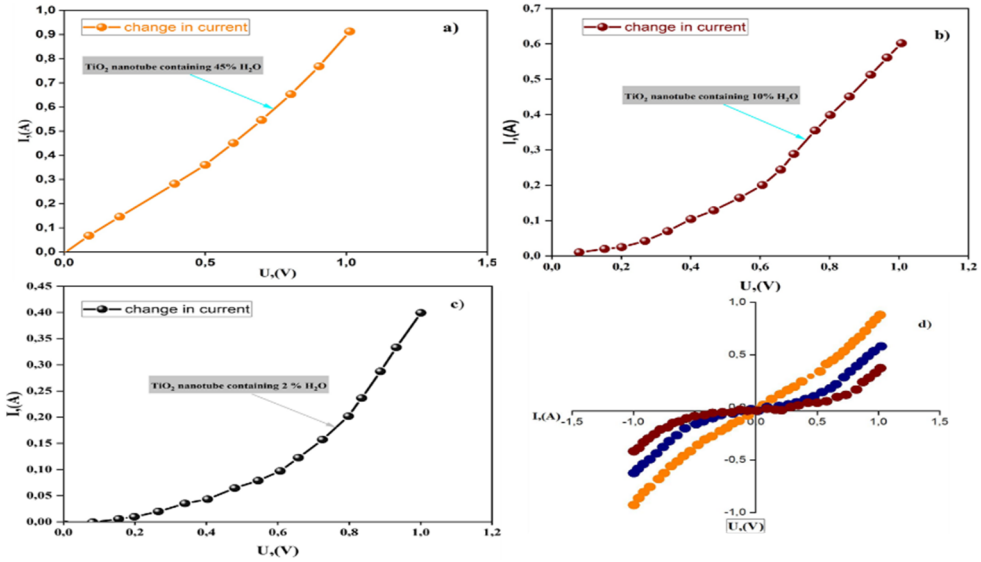

Fig. 10. Voltammetric characteristics of the obtained nanotubes electrolyte containing 45, 10 and 2 % water a-c and d their forward and reverse connection

Increasing the amount of water in the electrolyte solution leads to the formation of irregular nanotubes with reduced length and larger diameters. Variations in water content also significantly influence the electrical conductivity of the resulting nanocomposites. When a voltage of 0–1.5 V is applied, noticeable changes in the conductive state are observed (Fig. 10 a–b). This behavior is associated with the vertical direction of current flow, which can shift from positive to negative under the influence of the applied electric field and magnetic interactions, correlating with the formation of short, wide-diameter nanotubes.

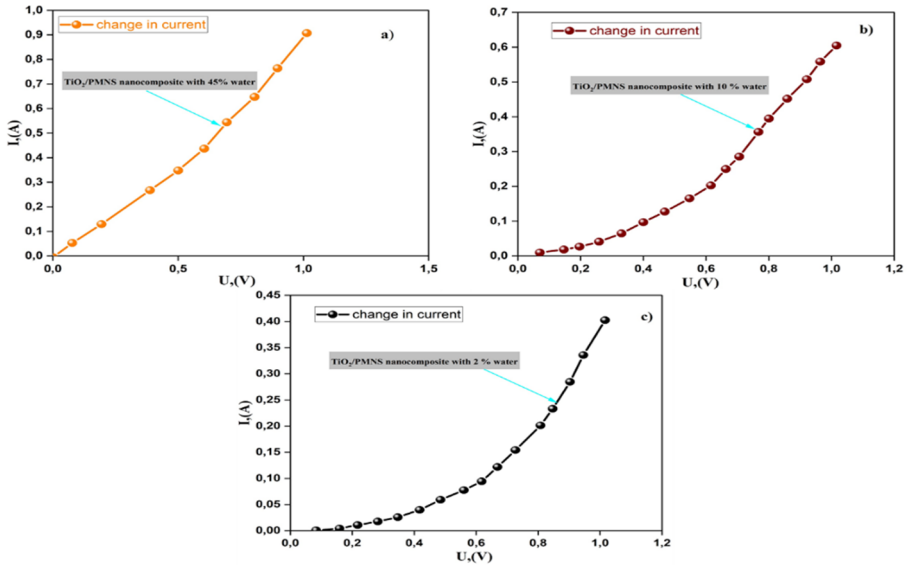

Fig. 11. Voltammetric characteristics of the obtained nanocomposites (with electrolyte contents of 45, 10 and 2 % water, a-c)

At lower water concentrations, the nanotubes formed are longer and exhibit narrower diameters, which results in improved conductivity compared to samples obtained from electrolytes with higher water content. Thus, the morphology of the nanotube array—specifically tube length and diameter—directly affects the electrical properties of the TiO_2/PMNS nanocomposites.

Fig. 10 c shows the volt-ampere characteristic of the forward and reverse connections, in which it can be seen that the current conductivity is improved when the contact is forward connected, and the current conductivity decreases when it is reverse connected.

The increase in the amount of current when the contact is forward connected and the decrease when the contact is reverse connected show that the current strength and voltage are directly proportional to each other.

It can be seen that the nanocomposites also have high conductivity at 0-1.5V (Fig. 11).

Conclusion

The volt-ampere characteristics and activation energies of the nanocomposites of the polymer obtained on the basis of naphthalene and its metal oxides with TiO_2 were determined. It was found that the electrical conductivity of polymethylenenaphthalenesulfonic acid is of the "p" type (positive), and its nanocomposites with metal oxides are of the "n" type (negative) conductive materials.

Currently nanocomposite materials can be used as structural components of electrode materials for rechargeable batteries and supercapacitors, as additives in the preparation of various antistatic composites, and as contact and current-conducting elements in control and measuring instruments.

References

1. Tomassi P., Buczko Z. *Aluminum anodic oxide AAO as a template for formation of metal nanostructures*. Electroplating of Nanostructures. 2015. Chapter. 318 p. DOI: 10.5772/61263
2. Sun X., Mo X., Liu L., Sun H., Pan C. Voltage-driven room-temperature resistance and magnetization switching in ceramic TiO_2/PAA nanoporous composite films. *ACS appl. mater&inter*, 2019, **Vol. 11(24)**, p. 21661-21667. DOI:10.1021/acsami.9b02593
3. Khamidov A., Hoshimov F., Butanov Kh., Mamatkulov Sh., Umarov B., Fang D., Sillanpää M., Pasquini L., Knauth Ph., Ruzimuradov O. Temperature-induced changes in pore structure and catalytic performance of aluminum oxide membranes. *Chemical Problems,* 2025, **Vol. 4(23),** p. 533-541. DOI: 10.32737/2221-8688-2025-4-533-541
4. Butanov Kh., Hoshimov F., Khamidov A., Mamatkulov Sh., Fang D., Ruzimuradov O. Pressure driven growth of In-Sn alloy nanowires in anodic aluminum oxide nanochannel: simulation and experimental study. *Bulletin of Chemical Reaction Engineering & Catalysis*, 2020, **Vol. 15**, p. 3. DOI: 10.2139/ssrn.4526435
5. Habazaki H., Fushimi K., Shimizu K, Skeldon P., Thompson G.E. Fast migration of fluoride ions in growing anodic titanium oxide. *Electrochemistry communications*, 2007, **Vol. 5**. p. 1222-1227.
6. Koleva G., Galabov B., Kong J., Schaefer H.F., Schleyer P. Electrophilic Aromatic Sulfonation with SO_3: Concerted or Classic SEAr Mechanism. *Journal of the American Chemical Society*, 2011, **Vol. 133(47),** p. 19094–19101. DOI:10.1021/ja201866h
7. De S.K. Aromatic Electrophilic Substitution Reactions. *Applied Organic Chemistry*, 2020. p. 293–321. DOI:10.1002/9783527828166.ch5
8. Li Z., Li Y., Li S., Wu J., Hu X., Ling, Z., Jin L. A modified quantitative method for regularity evaluation of porous AAO and related intrinsic mechanisms. *Journal of The Electrochemical Society*, 2018, **Vol. 165(5)**, DOI: 10.1149/2.0841805jes
9. Feng C., Zhang Z., Li J., Qu Y., Xing D., Gao X., Sun R. A bioinspired, highly transparent surface with dry style antifogging, antifrosting, antifouling, and moisture self-cleaning properties. *Macromolecular rapid communications*, 2019, **Vol. 40(6)**, 1800708. DOI: 10.1002/marc.201800708

10. Wang K., Liu G., Hoivik N., Johannessen, E., Jakobsen H. Electrochemical engineering of hollow nanoarchitectures: pulse/step anodization (Si, Al, Ti) and their applications. *Chem. Soc. Rev*, 2014, **Vol. 43(5)**, 1476. DOI: 10.1039/C3CS60150A
11. Lee K., Mazare A., Schmuki P. One-dimensional titanium dioxide nanomaterials: nanotubes. *Chemical reviews*, 2014, **Vol. 114(19)**, p. 9385-9454. DOI: 10.1021/cr500061m
12. Djumagulov Sh.Kh., Khamidov A.M., Todjiev J.N., Nurmanov S.E., Ruzimuradov O.N. Synthesis of nanocomposite materials and their properties based on polymethylene naphthylenesulfonate and TiO_2 nanotubes. *Austrian Journal of Technical and Natural Sciences*, 2024, **Vol. 11.** p. 28-37.
13. Kenjaev A.K., Nurmanov S.E., Khakberdiev Sh.M. Synthesis and properties of polymethylenenaphthalene sulfonic acid based on a secondary product of hydrocarbon pyrolysis. *Chemistry and Chemical Engineering*, 2024, **Vol. 2022(3)**, Article 8.
14. Li W., Zhang W., Li T., Wei A., Liu Y., Wang H. An Important Factor Affecting the Supercapacitive Properties of Hydrogenated TiO_2 Nanotube Arrays: Crystal Structure. *Nanoscale Research Letters*, 2019, **Vol. 14**, p.1-14. DOI: 10.1186/s11671-019-3047-2